27/1-18 A5 S5 (1)
I-1897
DR#0734-X

UCID-20141

# TRITIUM PERMEATION AND RECOVERY FOR THE HELIUM-COOLED MOLTEN SALT FUSION BREEDER

Albert E. Sherwood

September 1984

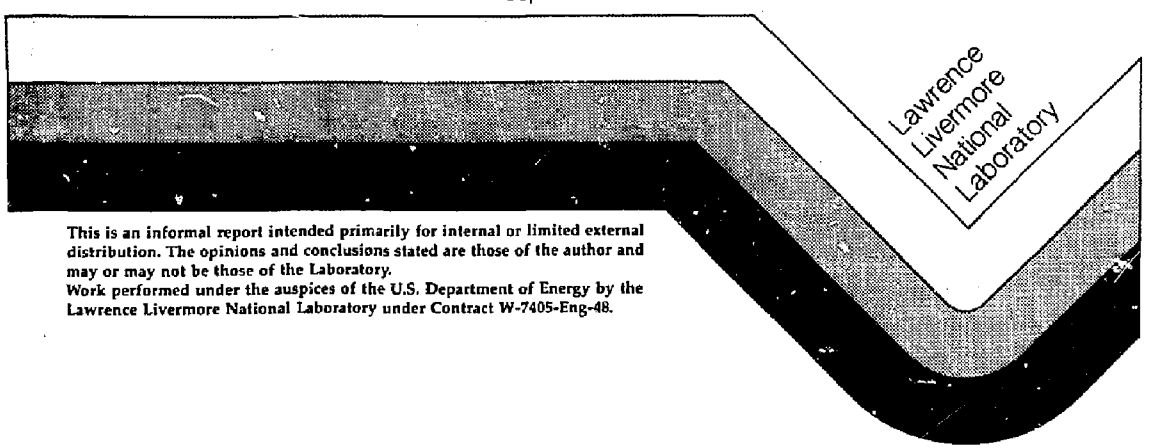


This is an informal report intended primarily for internal or limited external distribution. The opinions and conclusions stated are those of the author and may or may not be those of the Laboratory.
Work performed under the auspices of the U.S. Department of Energy by the Lawrence Livermore National Laboratory under Contract W-7405-Eng-48.

DISTRIBUTION OF THIS DOCUMENT IS UNLIMITED

UCID--20141

DE85 005304

# TRITIUM PERMEATION AND RECOVERY FOR THE HELIUM-COOLED MOLTEN SALT FUSION BREEDER

Albert E. Sherwood

Lawrence Livermore National Laboratory

Livermore, CA 94550

September 1984

**DISCLAIMER**

This report was prepared as an account of work sponsored by an agency of the United States Government. Neither the United States Government nor any agency thereof, nor any of their employees, makes any warranty, express or implied, or assumes any legal liability or responsibility for the accuracy, completeness, or usefulness of any information, apparatus, product, or process disclosed, or represents that its use would not infringe privately owned rights. Reference herein to any specific commercial product, process, or service by trade name, trademark, manufacturer, or otherwise does not necessarily constitute or imply its endorsement, recommendation, or favoring by the United States Government or any agency thereof. The views and opinions of authors expressed herein do not necessarily state or reflect those of the United States Government or any agency thereof.

MASTER

DISTRIBUTION OF THIS DOCUMENT IS UNLIMITED

## Abstract

Design concepts are presented to control tritium permeation from a molten salt/helium cooled fusion breeder reactor. This study assumes tritium to be a gas dissolved in molten salt, with TF formation suppressed. Tritium permeates readily through the hot steel tubes of the reactor and steam generator and will leak into the steam system at the rate of about one gram per day in the absence of special permeation barriers, assuming that 1% of the helium coolant flow rate is processed for tritium recovery at 90% efficiency per pass. Tritiated water in the steam system is a personnel hazard at concentration levels well below one part per million and this level would soon be reached without costly isotopic processing. Alternatives, including a combination of permeation barriers on reactor and steam generator tubes and molten salt processing, are estimated to reduce the leak rate into the steam system by over two orders of magnitude. For the option with the lowest estimated leak rate, 55 Ci/d, it may be possible to purge the steam system continuously to prevent tritiated water buildup. At best, isotopic separation of dilute tritiated water may not be necessary and for higher leak-rate options the isotopic processing rate can be reduced.

The proposed permeation barrier for the reactor tubes is a 10 μm layer of tungsten which, in principle, will reduce tritium blanket permeation by a factor of about 300 below the bare-steel rate. A research and development effort is needed to prove feasibility or to develop alternative barriers. The partial pressure of tritium gas dissolved in molten salt is high, easing the recovery process for which a flash-separator has been chosen. A 1 mm aluminum sleeve is proposed to suppress permeation through the steam generator tubes. This gives a calculated reduction factor of more than 500 relative to bare steel, including a factor of 30 due to an assumed oxide layer.

The permeation equations are developed in detail for a multi-layer tube wall including a frozen salt layer and with two fluid boundary-layer resistances. Conditions are discussed for which Sievert's or Henry's Law materials become flux limiters. An analytical model is developed to establish the tritium split between wall permeation and reactor-tube flow.

CONTENTS

## Nomenclature and Units

| | |
|---|---|
| $a$ | inner radius of frozen salt layer, m |
| $A$ | total reactor-tube area, $m^2$ |
| $A_j$ | area for helium/steam heat exchanger j, $m^2$ |
| $b$ | inner radius of steel reactor tube, m |
| $c$ | outer radius of steel reactor tube, m |
| $C_i$ | tritium concentration in material i, $Ci/m^3$ |
| $d$ | outer radius of coating (permeation barrier) or oxide layer, m |
| $D_i$ | diffusion coefficient for tritium in material i, $m^2/s$ |
| $D_{lm}$ | diffusion coefficient (molecular, not eddy) for tritium in molten salt, $m^2/s$ |
| $f$ | tritium flux, referred to inner tube radius b, $Ci/(s \cdot m^2)$ |
| $f(r)$ | tritium flux at radius r, $Ci/(s \cdot m^2)$ |
| $g$ | fraction of helium flow rate that is processed |
| $G$ | tritium volumetric generation rate, $Ci/(s \cdot m^3)$ |
| $H_i$ | Henry's Law coefficient for tritium in material i, $Ci/(m^3 \cdot Pa)$ |
| $i$ | subscript denoting material; see Fig. 2 |
| $I_i$ | inventory of tritium in material i, Ci or g |
| $j$ | subscript denoting helium/steam heat exchanger type |
| $k_i$ | boundary-layer mass transfer coefficient for tritium in fluid medium i, m/s |
| $K_{He}$ | Sievert's Law leak-rate coefficient through helium/steam heat exchanger tubes, see Eq. (58), $Ci/(s \cdot Pa^{1/2})$ |
| $K_{MS}$ | Sievert's Law leak-rate coefficient through molten salt reactor tubes, see Eq. (52), $Ci/(s \cdot Pa^{1/2})$ |

| | |
|---|---|
| $K'_{MS}$ | Henry's Law leak-rate coefficient through molten salt reactor tubes, see Eq. (54), Ci/(s•Pa) |
| $\ell$ | length of reactor tube, m |
| $L_{He}$ | Tritium permeation (leak) rate from helium system, see Eq. (57), Ci/s or Ci/d |
| $L_{MS}$ | Tritium permeation (leak) rate from molten salt reactor, see Eq. (49), Ci/s |
| $p$ | see $p(z)$ |
| $p(z)$ | tritium partial pressure in molten salt at axial location z, Pa |
| $p_i$ | tritium partial pressure in material i, Pa |
| $p_i(r)$ | tritium partial pressure at radius r in material i, Pa |
| $p_{max}$ | maximum tritium partial pressure in molten salt at tube outlet, see Eq. (36), Pa |
| $Q_5$ | flow rate of recirculating helium gas, $m^3/s$ |
| r | radial position in reactor tube, m |
| $S_i$ | Sievert's Law coefficient for tritium in material i, $Ci/(m^3 \cdot Pa^{1/2})$ |
| T | Temperature, K |
| U | mass-average velocity of molten salt in reactor tube, m/s |
| V | total irradiated molten-salt volume, $m^3$ |
| $W_j$ | steel wall thickness of helium/steam heat exchanger j, m |
| $y(z)$ | dimensionless tritium partial pressure at z, see Eq. (41) |
| z | axial location in reactor tube, measured from fluid inlet, m |
| $\alpha$ | fraction of generated tritium that permeates reactor tube wall |
| $\epsilon$ | partial-pressure drop ratio, see Eg. (23). Also: dimensionless wall-loss parameter, see Eq. (44) |
| $\eta$ | fractional recovery per pass through molten salt processor |
| $\eta_5$ | fractional recovery per-pass through helium slipstream processor |

## 1. Introduction

This report deals with tritium permeation and recovery from a molten salt/helium cooled fusion breeder reactor.[†] The design concept assumes that tritium is present as a gas dissolved in the molten salt, and that TF formation has been suppressed by reduction with $UF_3$. Doing this is both a blessing and a curse. On the blessing side, tube-wall corrosion from TF is suppressed, and the very high partial pressure of dissolved $T_2$ gas makes recovery relatively easy. Moreover, the desired fuel is recovered directly rather than an undesired and corrosive fluoride compound. On the negative side, tritium gas tends to permeate quite easily through steel walls at elevated temperatures, and a high tritium partial pressure makes the situation worse.

The production rate of tritium is 0.35 kg per day,[*] perhaps better expressed from a safety and environmental perspective as about 3 megacuries a day. To keep environmental losses low, say 30 curies/day, requires "5 nines" recovery - a .99999 recovery fraction! This can't be done from the molten salt alone and requires staged recovery; processing at least the molten salt and the intermediate helium coolant, and probably the steam/water system also.

To keep process rates down, distributed permeation barriers are needed to impede permeation between the fluid systems. Assuming the need to use stainless steel tubes for strength, permeation barriers will likely be applied as a coating or cladding on the steel tube walls. Tritium permeates through

[†]R. W. Moir et al., "Helium Cooled Molten Salt Fusion Breeder," Lawrence Livermore National Laboratory Report UCID-20153 (1984).

[*]The appropriate tritium consumption rate for 3000 MW of fusion power is 0.46 kg per day. We used 0.35 kg per day in this report. The leakage by permeation can be kept the same by increasing the barrier thickness somewhat. Also, the salt volume is 77 $m^3$ rather than the 65 $m^3$ used in this report.

all metals and, to a lesser extent, ceramics. We will focus here on the low-permeability metals. Figure 1 shows the temperature variation of the permeation coefficient of various low-permeability metals, including representative data for austenitic stainless steels for comparison[1]. A recent steel-alloy data survey[1a] recommends an equation for PCA (316 SS) which agrees with reference (1) within about 10 to 20% in the temperature range of interest. Table 1 gives the permeation-equation coefficients and literature references for Fig. 1, together with a numerical comparison of the permeation coefficients at 540°C. It can be seen that there is a dramatic improvement going down the list from steel towards tungsten, with the reduction exceeding four orders of magnitude for tungsten. There is some disagreement in permeation equations in the literature, especially for the lower permeability materials, and a recent review cites alternate literature sources[1b]. Beryllium is an exception, there can be no disagreement since there seems to be only one reference.

There are two reasons for wanting to keep tritium out of the steam system; the first reason is that any tritium leakage from there becomes a low-level environmental pollutant. This is a matter for concern, even though some consider it to be mainly a public-relations hazard. Tritiated water in the steam system, at seemingly low concentrations, can definitely be a personnel hazard as will be discussed in the next section.

In subsequent sections, we develop the permeation mathematics at some length. Our purpose is to show the somewhat subtle consequences that follow from combining the solubility laws of Sievert and Henry, and from the competing effects of permeation and forced convection.

A wide range of exploratory design options are then considered. These will need to be pruned down, assuming feasibility, based on considerations of safety,

ALARA, cost, etc. The intent is to show that there are many choices in tritium handling for this reactor concept. It is probably too early to focus on one favorite.

## 2. Tritium Toxicity

Some years ago, in an invited paper on the history of tritium, Willard Libby[7] referred to it as a "very benign isotope." His reasons were twofold: the 5.7 keV mean beta-decay energy is "one of the softest radiations known", and the 12.3 year half-life is short enough so that "we do not permanently contaminate the landscape." He then went on to express concern for tritium pollution from fusion power plants where the time scales of interest are less than the half-century or so needed for radioactive decay.

The words "benign" and "soft" are relative and can perhaps be misleading. Tritiated water vapor is readily absorbed by the human body via respiration or skin contact. A one Curie intake gives a whole-body dose of approximately 82 rem[3], half of which is delivered in the first week or two. Since pure $T_2O$ contains over 3000 Ci/cm$^3$, it can be argued that a drop of water constitutes a lethal dose. So $T_2O$ is certainly not "soft" water and Libby's friendly words do not apply, nor did he intend them to, until we dilute the tritium to trace levels with ordinary water.

On the other hand, tritium gas is virtually non-toxic, at least as long as you can hold your breath. Even if inhaled, disintegrating gas atoms deliver a relatively mild dose to lung tissue and most of the rest are exhaled with only about 0.01% retained as tritiated water[8]. So perhaps tritium gas might fairly be called "benign." An important question is how fast tritium gas converts to water in the presence of water vapor and oxygen. Unfortunately,

there is no simple answer. The conversion half-time can range from seconds on a catalytic surface [9] to years [10] in a Pyrex flask.

Tritium that is not recovered by processing in the molten-salt and helium-coolant loops will enter the steam system where it will tend to accumulate as tritiated water. Will this water be benign or hazardous? For permeation scenarios to be discussed below, we might expect HTO concentration to rise to, say, 1 Curie/liter. This corresponds to less than one part per million and could be considered a low level of contamination by ordinary standards. Let's assume a confined working area where a small amount of water leaks from the steam system and reaches equilibrium with water vapor in the air at 25C. A worker breathing this air will be exposed at the rate of about 3 rem/h,* i.e., that person will reach the 1 rem annual occupational dose limit in only 20 minutes. Any leakage from a 1 Curie/liter tritiated water system is definitely going to represent a serious personnel hazard. For this reason alone, it is desirable to design permeation barriers and processing that will minimize the tritium input into the steam loop. In contrast, a small amount of leakage from the helium-coolant loop will not be as hazardous to personnel, assuming that tritium present there is mainly in the hydrogen-gas form.

## 3. Tritium Partial-Pressure Distribution in a Multi-Layer Cylindrical Wall

Fig. 2 shows the permeation geometry near the wall of a molten-salt reactor tube in radial cross report. One might approximate the radial geometry with

*Based on equilibrium HTO vapor concentration of 0.023 Ci/$m^3$ and a dose conversion factor[8] of 130 (rem/h)/(Ci/$m^3$).

a slab; instead we solve the problem exactly and then introduce approximations. Five material regions are included: 1- molten salt in the central region of the tube, 2- a frozen salt layer at the inner wall of the tube, 3- the stainless steel tube itself, 4- a coating or oxide layer at the outer wall, 5- and helium gas outside the tube. In addition, we allow boundary layers of finite mass-transfer resistance, but with negligible thickness, at the two fluid/solid interfaces. These represent the mass-transfer analog of a thermal boundary layer in heat flow. Boundary-layer thickness must, of course, be finite and will depend on fluid properties, mainly the Reynolds Number. The mass transfer coefficient incorporates the boundary-layer thickness since it is, like the heat-transfer coefficient, a lumped parameter.

## 3.1 Derivation of Steady-State Permeation Equations Without Axial Flow

Assume that tritium is generated at a constant rate G per unit volume in regions 1 and 2, and that the mass flow is radial and at steady state. Neglect radioactive decay compared to production. The time constant to reach steady state is about an hour for steel tube at 500°C, and roughly a day at 300°C. Assume Fick's Law diffusion in regions 1-4, and assume the helium in region 5 is well-mixed due to turbulent flow. We will eventually examine the mixing in the molten salt region; for now, assume a finite diffusivity in region 1.

For simplicity, we write the equation for mass conservation in the same form for regions 1-4:

$$r^{-1}d[D_i r(dC_i/dr)]/dr + G_i = 0 \ , \ i = 1, 2, 3, 4 \qquad (1)$$

where

$$G_i = \begin{cases} G, & i = 1, 2 \\ 0, & i = 3, 4 \end{cases} \tag{2}$$

$C_i = C_i(r)$ is the tritium concentration in region i at radius r. Diffusivity, $D_i$, is a function of temperature and therefore implicitly a function of radius through the steady-state temperature profile; $D_i = D_i[T(r)]$. One can define an appropriate average $D_i$ by means of the first integral of Eq. (1), and we will interpret $D_i$ in this averaged sense.

The four constants that arise from the first integral of Eq. (1) are found by applying the following boundary conditions; the concentration gradient is zero at the center of the tube, and the flux, $-D_i[dC_i/dr]$, is continuous at radius a, b, and c. The interface fluxes turn out to be:

$$f(a) = Ga/2 , \tag{3}$$

$$f(b) = Gb/2 , \tag{4}$$

$$f(c) = bf(b)/c , \tag{5}$$

$$f(d) = bf(b)/d , \tag{6}$$

and the concentration profiles may be written:

$$C_1(r) = C_1(a) + G(a^2 - r^2)/(4D_1), \quad 0 \leq r < a, \tag{7}$$

$$C_2(r) = C_2(b) + G(b^2 - r^2)/(4D_2), \quad a < r < b, \tag{8}$$

$$C_3(r) = C_3(c) + Gb^2 \ln(c/r)/(2D_3), \quad b < r < c, \tag{9}$$

$$C_4(r) = C_4(d) + Gb^2 \ln(d/r)/(2D_4), \quad c < r < d. \tag{10}$$

The result, so far, is the same as the solution to the steady heat-flow problem. If we were considering heat flow, we would next assume local thermal equilibrium at material interfaces and equate interface temperatures. For

diffusion, we instead assume local chemical equilibrium at interfaces and equate the chemical potentials of the diffusing substance. Since chemical potential is linear in the logarithm of partial pressure for an ideal gas, we can equate interface partial pressures:

$$p_i = p_{i+1} , \qquad i = 1,2,3,4. \tag{11}$$

If tritium remains a diatomic gas upon dissolving in a particular material, then the equilibrium concentration is related to the gas phase partial pressure by Henry's Law:

$$C_i = H_i p_i , \tag{12}$$

where $H_i$ is a temperature-dependent solubility constant and $p_i$ is tritium gas partial pressure. This linear relation between concentration and partial pressure always holds at low concentrations, provided that dissociation or other chemical reaction does not occur[11]. For example, the solubility of hydrogen and deuterium in molten $Li_2BeF_4$ obeys Henry's Law[12]. In contrast, the solubility of hydrogen isotopes in metals obeys Sievert's Law:

$$C_i = S_i \sqrt{p_i} , \tag{13}$$

where $S_i$ represents Sievert's constant. This square-root relation follows from thermodynamic arguments if gas-phase tritium is completely undissociated and solid-phase tritium is completely dissociated into atoms. Intermediate cases of partial dissociation in the gas-phase[13] and in the condensed-phase [14] have been considered, and the relation between concentration and partial pressure is not as simple as in the limiting case of Henry's or Sievert's Law.

We assume Henry's Law applies for tritium in molten and frozen salt, and also in helium, while Sievert's Law applies in steel and the coating or oxide layer on the steel. Note that solubility constants are, in general, different for each material. This implies a discontinuity in concentration at material interfaces, even those without fluid boundary layers. Across a boundary layer we have an additional concentration change:

$$\Delta C_i = f/k_i \ , \tag{14}$$

where f represents the local mass flux, and $k_i$ is a mass transfer coefficient. By means of Eqs. (11)-(14), we can solve for the four unknown interface concentrations in Eqs. (7)-(10). Expressing the results, for convenience, as interface partial pressures gives:

$$p_1(a) = f(a)/(k_1H_1) + G(b^2 - a^2)/(4D_2H_2) + p_2(b) \ , \tag{15}$$

$$p_2(b) = [Gb^2\ln(c/b)/(2D_3S_3) + \sqrt{p_3(c)}]^2 \ , \tag{16}$$

$$p_3(c) = [Gb^2\ln(d/c)/(2D_4S_4) + \sqrt{p_4(d)}]^2 \ , \tag{17}$$

$$p_4(d) = f(d)/(k_5H_5) + p_5 \ , \tag{18}$$

where $p_5$ represents tritium partial pressure in well-mixed helium gas.

Finally, the tritium partial pressure profile at any radial position follows from Eqs.(7)-(10) as:

$$p_1(r) = p_1(a) + G(a^2 - r^2)/(4D_1H_1) \ , \qquad 0 < r < a, \tag{19}$$

$$p_2(r) = p_2(b) + G(b^2 - r^2)/(4D_2H_2) \ , \qquad a < r < b, \tag{20}$$

$$p_3(r) = [\sqrt{p_3(c)} + Gb^2\ln(c/r)/(2D_3S_3)]^2 \ , \quad b < r < c, \tag{21}$$

$$p_4(r) = [\sqrt{p_4(d)} + Gb^2\ln(d/r)/(2D_4S_4)]^2 \ , \quad c > r > d. \tag{22}$$

The set of eight equations listed above constitutes a formal solution to the problem of steady-state radial diffusion through four material regions having different properties, with generation in the two innermost regions, and with boundary-layer resistance at the two fluid/solid interfaces.

### 3.2 Comparison of Mass-transfer Resistances in Molten Salt

Since the solid regions will have thin walls, the radial dependence given by Eqs.(20)-(22) will not be needed for most calculations. Equation (19), on the other hand, applies to molten salt over the entire central region of the tube from centerline to the boundary layer at radius a. It is of interest to estimate the partial pressure change across this region and compare it with the drop across the boundary layer. Define $\epsilon$ as a ratio of partial-pressure drops:

$$\epsilon = [p_1(0) - p_1(a)]/[p_1(a) - p_2(a)] \ . \qquad (23)$$

Using Eqs. (3), (15), (19), and (20) it follows that

$$\epsilon = ak_1/(2D_1) \ . \qquad (24)$$

We know intuitively that in highly turbulent flow the molten salt will be well mixed, which amounts to saying that the effective diffusivity, $D_1$, must be large and that $\epsilon$ will be a small number. Even in the absence of axial flow, we expect some natural convection due to the high heat generation and associated temperature gradients in the molten salt. Suppose, conservatively,

that the natural circulation velocity is small and generates only a lazy, laminar flow. For this case, the mass transfer coefficient is:

$$k_l = 2D_{lm}/a \ , \qquad (25)$$

where $D_{lm}$ represents the molecular diffusivity of $T_2$ in molten salt. Equation (25) is equivalent to a heat transfer Nusselt number of 4, a value which is correct to one digit for laminar flow[15]. For $D_l$, we use the laminar-flow axial dispersion coefficient:

$$D_l = D_{lm} + (Ua)^2/(48D_{lm}) \ , \qquad (26)$$

where U is the mean flow velocity[16]. We do not know of any measurements of $T_2$ diffusivity in molten Flibe, with or without a $ThF_4$ loading. However, Katsura and Furukawa [17] have measured the diffusivity of $H_2$ in molten Flinak, and we use their result:

$$D_{lm}[m^2/s] = (7.0E\text{-}06)\exp(-4530/T[K]) \ . \qquad (27)$$

With a 1/2 inch tube at 600°C, and with an assumed velocity of 1 mm/s, the pressure drop ratio, $\varepsilon$, turns out to be $2 \times 10^{-3}$. For all practical purposes, we can assume the tritium partial pressure in the molten salt is uniform from the tube centerline out to the fluid/solid boundary layer where there is a sudden discontinuity. Equation (19) has now served its purpose, and the four interface Eqs. (15)-(18) are all we need for calculations.

### 3.3 Tritium Partial-Pressure Profiles Without Molten Salt Processing

In order to make use of the results of the last section, a large number of parameters must be estimated. Many of these are temperature sensitive, especially diffusivity and solubility which depend exponentially on temperature. We first establish the thermal profile for a tube with given heat generation rate, outside helium temperature, etc. Table 2 shows the calculated results for three reactor tubes located at 1.5, 1.8, and 2.1 m from the plasma centerline, where the local heat generation rates are 60, 20, and 6 $MW/m^3$. Calculated temperatures and frozen salt layer thickness are sensitive to tube location. Other parameters such as the helium boundary-layer film coefficient can also change the results. Table 2 is based on a 1/2 inch tube. Tailoring the tube size to radial position may be a useful way to adjust the thermal profile and frozen layer thickness.

Table 3 shows tritium permeation calculations based on the thermal profiles established in Table 2, and without axial flow so that all generated tritium permeates through the wall. The frozen salt layer is assumed to have the same diffusion and solubility parameters as molten salt with $D_1$ and $D_2$ given by Eq. (27) and Henry's Law solubility[12] expressed by:

$$H_1[Ci/(m^3 \cdot Pa)] = H_2 = 1.19 \times \exp(-3530/T[K]) \qquad (28)$$

The molten salt boundary-layer mass transfer coefficient, $k_1$ is estimated by means of Eq. (25) i.e., based on laminar flow. A nominal 1 μm tungsten coating is used for region 4. Permeation coefficients for tungsten and steel are as given in Table 1. The helium boundary-layer mass transfer resistance turns out to be negligible at an assumed Reynolds number of 3000.

The main point of Table 3 is to show that, for a fixed tube geometry, the tritium partial-pressure distribution can be significantly altered by tube location. This is due to changes in the generation rate and the temperature distribution. It is also interesting to note the change of the relative permeation resistance of different portions of the multi-layered wall. This behavior is unlike relative thermal resistances in heat flow which are nearly independent of the flux. If we had chosen to use, say, a 10 um tungsten coating rather than 1 μm then the tungsten barrier would have been the dominant permeation resistance under all conditions. Note that neither the steel tube nor the frozen salt layer offer very much help, while the molten salt resistance can be significant based on the small mass transfer coefficient in laminar flow. We may have understated the frozen salt-layer resistance, since one would expect the solid to have a lower diffusivity than the liquid. The diffusivity of tritium in both solid and liquid Flibe will certainly need to be measured as this reactor concept is developed. Even if the frozen-layer diffusivity was much smaller, it seems unwise to count on a dynamic layer that is sensitive to thermal alteration and disruption for other reasons, e.g. periodic blowoff due to helium buildup.

For design calculations below, we will therefore consider only two simple extremes where the permeation resistance is dominated either by molten salt alone or by a tungsten barrier. Also, the material temperatures in Table 2 for the intermediate tube at 1.8 m from the plasma centerline (20 $MW/m^3$) will be taken as representative for design calculations since the tritium generation rate for this tube is not far from the reactor-mean generation rate; G = 0.596 $Ci/(s \cdot m^3)$.

We should emphasize two important messages gained from Tables 2 and 3:

(1) Although we know the reactor-mean tritium generation rate, we do not have a corresponding mean tube-wall temperature distribution such that permeation from a representative tube will represent the correct integrated average over the whole assembly.

(2) Even if we did, the change in relative importance of wall resistance terms for tubes at different locations implies that exploratory calculations for a "representative" tube should be scaled to other conditions with caution.

### 3.4 Radial Flux Equation for Tritium

If molten salt is flowing in the reactor tube, then the radial tritium flux is not proportional to production rate G, as in Eqs. (3)-(6), and instead depends on the local tritium concentration in molten salt and other system parameters. We will focus on the flux at b, the inner radius of the steel tube, and from now on denote f(b) as f. We will assume the local tritium concentration is well mixed, as previously discussed, and denote $p_1(a)$, the tritium partial pressure in the salt, as p. From Eqs. (15)-(18), replacing G by means of Eq.(4), we can write

$$p = fa/(bk_1H_1) + f(b^2 - a^2)/(2bD_2H_2) +$$

$$+ [fb\ln(c/b)/(D_3S_3) + fb\ln(d/c)/(D_4S_4) + \sqrt{fb/(dk_5H_5) + p_5}]^2 \quad . \quad (29)$$

Eq. (29) cannot be solved explicitly for f. This is typical of realistic permeation conditions with multiple layers where Henry's Law and Sievert's Law regions are coupled.

Consider two simplified cases; where the permeation resistance is dominated either by the molten salt, or by the coating. For the case of molten-salt resistance only, neglecting $p_5$ and assuming thin walls, solving Eq. (29) for f gives

$$f \simeq [2D_{1m}H_1/b]p \ , \tag{30}$$

where we have assumed the laminar-flow approximation of Eq. (25) for $k_1$. For the case of coating resistance only, the flux is given by:

$$f \simeq [D_4S_4/(d-c)]\sqrt{p} \ . \tag{31}$$

Note that the tritium flux is directly proportional to partial pressure when the material with the limiting permeation resistance has a Henry's Law solubility, while the flux is proportional to the square root of partial pressure for a Sievert's Law material. The net effect is to make the Sievert's Law material the flux limiter if tritium partial pressure is high, and the Henry's Law material the flux limiter at low partial pressures. Table 3 illustrates these two extremes as well as the intermediate case where both materials serve to impede the flux.

4. Tritium Split Between Wall-Permeation and Reactor-Tube Flow

We want to remove most of the tritium before it permeates through the reactor tube walls into the helium coolant. To do this, the molten salt must be circulated rapidly through an external process unit where tritium can be recovered. For now, we will take it for granted that a recovery system can be

designed and focus on the required permeation characteristics and recirculation rate needed to guarantee that only a small fraction of generated tritium will permeate the tube walls.

## 4.1 Model Assumptions and Mass-Balance Integral over Reactor Tube

As discussed earlier, tritium tends to mix well in the molten salt due simply to natural convection. Good mixing is reasonable on a length scale of the order of the tube size. To model the behavior of flow in a long tube, we assume that tritium is well-mixed radially while the partial pressure changes continuously in the axial direction z, that is:

$$p = p(z) \ . \tag{32}$$

Let U represent the mean velocity along the z axis. As before, G is the volumetric generation rate, f is the local permeation flux, and $H_l$ is Henry's constant for molten salt. A mass balance on a differential volume element, as sketched in Fig. 3, yields:

$$-UH_l dp/dz - 2f/b + G = 0 \ . \tag{33}$$

Steady state is assumed, and axial diffusion has been neglected on the grounds that it is small compared to the bulk transport. Rearranging Eq. (33) and integrating over the tube from the molten salt inlet at 0 to the outlet at $\ell$ gives:

$$H_l \int_{p(0)}^{p(\ell)} [G - 2f/b]^{-1} \, dp = \ell/U \ . \tag{34}$$

This expression can be integrated numerically to find outlet pressure $p(\ell)$ for the general case, discussed in the last section, where f is not a simple function of the tritium partial pressure. The tube inlet pressure $p(0)$ is related to $p(\ell)$ by

$$p(0) = (1-\eta)p(\ell) \quad , \tag{35}$$

where $\eta$ represents the single-pass recovery fraction in the molten salt processing loop. For the limiting case of perfect containment, we can calculate the maximum tritium pressure at the tube exit by integrating Eq. (34). Let's call this pressure $p_{max}$:

$$p_{max} = G\ell/(nH_1U) \quad . \tag{36}$$

We are interested in the escape fraction $\alpha$, which represents the fraction of tritium generated in the tube that escapes through the wall before leaving the tube. An overall mass balance tells us that:

$$\alpha = 1 - p(\ell)/p_{max} \quad . \tag{37}$$

## 4.2 Tritium Escape Fraction with a Henry's Law Barrier as Flux Limiter

For the special case of the linear flux-pressure relation in Eq. (30) with only molten salt resistance, the result of integrating Eq. (34) and then solving for the escape fraction by means of Eq. (37) is

$$\alpha = 1 - (\eta/\nu)[1 - \exp(-\nu)]/[1 - (1-\eta)\exp(-\nu)] \quad , \tag{38}$$

with parameter $\nu$ defined as:

$$\nu = 4D_{lm}b^{-2}\,\ell/U \quad . \tag{39}$$

If the permeating fraction is to be small, then we must have $\nu \ll 1$, in which case the exponentials can be expanded, and then $\alpha$ is simply:

$$\alpha = \nu[1/2 + (1-n)/n] + \ldots \quad . \tag{40}$$

The ratio of tube length to mean velocity, $\ell/U$, that appears in parameter $\nu$ represents the residence time of fluid passing through a tube, in other words the ratio of fluid volume to volumetric flow rate for that tube. If we neglect variations in tube length at different radii and possible variations in tube diameter, then tube residence time also represents the ratio of total molten salt volume to total volumetric flow rate. Nominal tube length varies from 9 to 13 m, with an average of, say, 12 m. There will be additional manifolding length, which we will neglect since it will not be part of the 65 $m^3$* design-basis volume of molten salt in the reaction zone. We pick a velocity of 0.1 m/s, which corresponds to a tube Reynolds number of about $3 \times 10^2$. The tube residence time, on this basis, is 2 minutes and the total volume flow rate of molten salt is 0.54 $m^3/s$ (8600 GPM). Assuming a recovery fraction of 0.9, and calculating molten salt diffusivity based on a temperature of 680°C gives $\nu = 0.86$. Using the exact analytical solution for $\alpha$, since $\nu$ is not small in this case, the fraction of generated tritium that escapes through the tube walls is 0.37. This 37% loss could be reduced to a 15% loss

*The salt volume in the fusion breeder report is 77 $m^3$ rather than 65 $m^3$ used here.

by increasing the velocity by a factor of three. The processing rate would then be 1.6 $m^3/s$ (26000 GPM), which is starting to become uncomfortably high.

4.3 Tritium Escape fraction with a Sievert's Law Barrier as Flux Limiter

Define a normalized pressure y(z) at any position z along the tube axis:

$$y(z) = p(z)/p_{max} \ . \tag{41}$$

We assume that the coating-resistance term dominates in the general flux relation, Eq. (29), in which case the wall flux is given by:

$$f = D_4 S_4 \sqrt{p}/[b\ell n(d/c)] \ . \tag{42}$$

This equation reduces to Eq. (37) in the thin-wall approximation, a step which will be deferred for now since one might wish to consider a wide range of coating thicknesses. After substituting flux Eq. (42) into the integral in Eq. (34), the resulting integral equation can be written:

$$\int_{(1-n)y(\ell)}^{y(\ell)} [1 - \epsilon \sqrt{y}\ ]^{-1} \, dy = n \ , \tag{43}$$

where the dimensionless wall-loss parameter $\epsilon$ is defined by:

$$\epsilon = 2D_4 S_4 \sqrt{p_{max}}/[b^2 \ell n(d/c) G] \ , \tag{44}$$

and all other symbols have been defined. We should note that the operational

parameter of direct interest to us, i.e., the tritium escape fraction, is related simply to $y(\ell)$ by:

$$\alpha = 1 - y(\ell) \ . \tag{45}$$

The point in writing Eq. (43) in the particular form given above, is as follows. First of all, we note that it can be integrated exactly but the result is transcendental in $y(\ell)$ and thus rather opaque for computational purposes. So we resort to a series expansion of the integrand followed by term-by-term integration. We proceed by noting that $\epsilon$ is a small number, generally much less than unity for the low-permeability materials of interest to us. The varible y is also less than unity, and so we can expand the integrand of Eq. (43) in the form

$$[1 - x]^{-1} = 1 + x + x^2 + \ldots \ . \tag{46}$$

Keeping only the first two terms, integrating, and solving for the tritium escape fraction gives:

$$\alpha = 2[1 - (1-\eta)^{3/2}]\epsilon/(3\eta) + \ldots \ . \tag{47}$$

We can see that $\epsilon$ is roughly equal to $\alpha$, and since we are going to demand that $\alpha$ be small, it follows that our expansion to terms of order $\epsilon$ will be accurate.

Combining Eqs. (36), (44), and (47) gives the final working equation for tritium escape fraction for a Sievert's Law flux limit, in terms of all the system parameters:

$$\alpha = (4/3)n^{-3/2}[1 - (1-n)^{3/2}]b^{-2}[\ell/K_1G]^{1/2}D_4S_4/[U^{1/2}\ell n(d/c)] \quad . \qquad (48)$$

The permeation coefficient $D_4S_4$ has the most important effect since it varies by orders of magnitude among materials. Once the material is specified, the main variables in process design are wall thickness, velocity, and process recovery efficiency. Although it's a little hard to see in Eq. (48), the product nU is nearly constant at fixed $\alpha$, and so a decrease in process efficiency can be compensated by a corresponding increase in flow velocity.

Evaluating the above expresssion using a 10 μm tungsten coating at 540 C, with other parameters the same as the previous linear case, gives a calculated escape fraction equal to 0.08. The 10 μm tungsten barrier reduces the permeation rate below that of the 20 mil bare stainless tube by a factor of about 300. This is a substantial improvement, yet not so high as to defy credibility. Coatings are inevitably imperfect. Asking for a permeation reduction factor of 300 over the base metal implies that an uncoated portion (cracks, pinholes, etc.) of only about 1 part in 1000 of the bare tube area can be tolerated without degrading performance. To do the same job with beryllium requires a 64 μm layer, based on Table 1. Gold is next in line in permeability and is an easily applied, non-brittle coating material. Unfortunately, to match 10 μm of tungsten would require an 0.65 mm layer of gold and cost about $4 billion! The effectiveness of tungsten or other low-permeability barriers must be assessed by an experimental research and development program. Tungsten powder can be melted and applied to tube exteriors by a commercial plasma-spray process. Tungsten can also be coated on surfaces by chemical vapor deposition from the volatile hexafluoride[18], which might permit the inside of the reactor tubes to be coated as well.

## 5. Tritium Permeation Rate to Helium Coolant Loop for Three Design Options

The essential results of the last section are contained in Eqs. (38) and (48) for tritium escape fraction in the Henry's or Sievert's Law flux limit. The leak rate (permeation rate) of tritium from the molten salt loop is the product of escape fraction, volumetric production rate, and total molten-salt volume in the reactor tubes:

$$L_{MS} = \alpha G V \quad . \tag{49}$$

For both the Henry's and Sievert's Law cases assuming, as usual, a small escape fraction, the outlet tritium partial pressure is, to a good approximation, given by Eq.(36), $p_{max} = G\ell/(nH_1U)$, and by using this relation we can write the permeation rate in a more familiar fashion in terms of partial pressure. The total tube area A, can also be introduced by recognizing that

$$A = 2V/b \quad . \tag{50}$$

For a Sievert's Law barrier as flux limiter, assuming a thin-walled tube, Eq.(49) can be written

$$L_{MS} = K_{MS}\sqrt{p_{max}} \quad , \tag{51}$$

where the Sievert's Law leak-rate coefficient from the molten-salt loop $K_{MS}$ is:

$$K_{MS} = \{(2/3n)[1 - (1-n)^{3/2}]\}D_4S_4A/(d-c) \quad . \tag{52}$$

the terms following the curly bracket are what we would expect in a permeation equation; diffusivity, solubility, area, and wall thickness. If we had ignored the axial gradient and assumed the tube was a well-mixed tank, as will be done in the helium section to follow, the result turns out to look exactly like the above except that the quantity in the curly brackets is unity. This factor, which depends only on process efficiency, is the correction for the axial gradient due to the tritium processor which recycles molten salt with a low tritium partial pressure back to the reactor tube inlet.

Going through a similar procedure for a Henry's Law barrier as the flux limiter, the leak rate can be written

$$L_{MS} = K'_{MS}P_{max} \quad , \tag{53}$$

where Henry's Law leak-rate coefficient $K'_{MS}$ is:

$$K'_{MS} = \{1 - n/2\}k_1H_1A \quad , \tag{54}$$

and, again, the curly-bracket factor represents the axial-gradient correction to a well-mixed-tank model.

We now consider some design alternatives which cover a range of feasible options:

Option A - process molten salt, restrict permeation

Option B - process molten salt, unrestricted permeation

Option C - no salt processing, 100% permeation

A 10 μm tungsten barrier (as discussed in the paragraphs following Eq. (48)) is used in case A, while cases B and C have only the molten salt boundary-layer resistance. The process recovery fraction is 0.9 for cases A and B, while case C has no tritium recovery system for the molten salt. The temperatures for permeation are 540 and 680°C for tungsten and molten salt, respectively. Other parameters are given in Table 4 along with calculated results. For case A, Eq. (51) is used for the leak rate. For case B, the leak rate is too large for Eq. (53) to be accurate, instead Eq. (49) is used along with Eqs. (38) and (39) which gives the exact solution to the linear problem. For case C, the tritium pressure in molten salt is obtained from Eq. (29) rather than Eq. (36). The leak rate to the helium loop is 7.6%, 37%, and 100% for case A, B, and C, respectively.

## 6. Tritium Permeation into the Steam/Water Loop

From the point of view of tritium permeation, the helium-coolant loop is in a crucial position; between the molten salt and steam systems. Figure 4 shows a sketch of the three tritium processing loops. Tritium is generated at a high rate in the molten salt and it will be difficult to recover much more than 90% of the tritium produced there. Tritium that permeates through the reactor tubes will enter the helium heat-transfer loop. Table 5 gives approximate figures on amounts and flow rates in the three loops. The mass of molten salt is large, due to its high density. However, pumping power and equipment size and cost scale with volumetric flow rate. The bottom line on Table 5 shows why it is unreasonable to process, for tritium recovery, more than a small fraction of the helium flow which amounts to 800 $m^3/s$ (nearly 2 million ACFM) @ 450°C and 60 atm.

A steady-state concentration will quickly be reached which will depend on the helium volume and helium-processing rate, assuming that processing is the main removal mechanism. There will also be a tritium permeation loss through the walls of the helium/steam heat exchanger, and perhaps some conversion of tritium gas by homogeneous-phase oxidation to water or chemical exchange with water vapor in the circulating helium. Direct conversion in the helium is an intriguing possibility, and Maroni[20] has presented the thermodynamic arguments which tell us that tritium gas partial pressure (and therefore the permeation loss) will be very small if a modest oxygen partial pressure is maintained and tritiated water vapor is adsorbed at a reasonable rate, assuming equilibrium prevails. Unfortunately, the kinetics are too slow without a catalyst and a conventional catalytic converter to handle 800 $m^3/s$ would be absurdly large. The design challenge is to get a large catalytic surface area into the helium without introducing any significant pressure drop; e.g., $10^3$Pa at 800 $m^3/s$ requires 1 MWe of pumping power at 80% efficiency. Perhaps very small catalytic particles could be distributed and maintained in the flowing gas. For design calculations below, we will simply use a conventional catalytic reactor in a relatively low-flow bypass loop.

## 6.1 Permeation Rate Equation for Well-Mixed Tank Model

For this study, we will assume that tritium entering the helium system is either recovered in a helium slipstream processor or permeates to the steam system, in which case the mass balance reads:

$$L_{MS} = n_5 g Q_5 H_5 p_5 + L_{He} \cdot \qquad (55)$$

The fractional efficiency of slip stream processing is $\eta_5$, the fraction of helium that is processed is g, $H_5$ and $p_5$ are the Henry's Law constant and partial pressure for tritium in helium, and $L_{He}$ is the permeation rate out of the helium system. The assumption of a well-mixed tank is implicit in the above equation. Assuming that $L_{He} << L_{MS}$, we neglect the second term in Eq.(55) and solve for the tritium partial pressure

$$p_5 = L_{MS}/(\eta_5 g Q_5 H_5) \quad . \tag{56}$$

The leak rate $L_{He}$ is assumed to depend only on the helium-side partial pressure

$$L_{He} = K_{He}\sqrt{p_5} \quad , \tag{57}$$

where $K_{He}$ is a Sievert's Law leak-rate coefficient for the helium/steam heat exchanger tubes.

Table 6 shows heat exchanger design data for the reactor of reference [19], which we have combined with permeation data[1] for clean, unoxidized stainless steel to give a leak rate per unit driving force. It is interesting to note that there is a considerable difference in the mean wall temperature of the four types of exchangers shown in Table 6. We define the mean wall temperature as the arithmetic average of helium and steam/water inlet and outlet temperatures. As a consequence of this temperature difference, the resuperheater accounts for 46% of the leakage although it has only 15% of the wall area and, in addition, thicker walls.

The overall leak-rate coefficient is calculated from

$$K_{He} = \sum DS_j A_j / W_j \quad , \tag{58}$$

where the sum is over each heat exchanger with specified permeation coefficient $DS_j$, area $A_j$, and wall thickness $W_j$.

## 6.2 Permeation Rates into Steam for a Range of design Options

Two design alternatives are considered for the helium/steam heat exchanger system:

option 1 - restrict permeation with a 1 mm aluminum sleeve

option 2 - unrestricted permeation

Unrestricted permeation (see Fig. 2) means that the only resistance comes from the stainless steel tube wall (material 6 present, material 7 absent), while restricted permeation implies that the aluminum permeation barrier (material 7) is present and is the tritium flux limiter.

For option 2 a steel tube leak-rate coefficient of 1.44E+4 $Ci/(d \cdot Pa^{1/2})$ is used. This is obtained from the temperature- and area-averaged coefficient given in Table 6 by dividing by a factor of 10 to allow for an oxide layer on the steam side. This is believed to be a conservative oxide-factor "credit." Much higher factors have sometimes been reported, but the effective permeation reduction by thin oxide layers is rather uncertain. We have ignored fluid boundary-layer resistances for these heat exchangers.

For option 1 we use a 1 mm aluminum sleeve as permeation barrier with the sleeving assumed to slip inside the steel tubes of option 2. Such laminated tubes will require development to ensure good thermal contact. Aluminum has a larger thermal expansion coefficient than steel. The same temperatures and areas in Table 6 are used, as a simplifying approximation. The aluminum

sleeve leak-rate coefficient is 269 Ci/(d•Pa$^{1/2}$), obtained from the Table 1 data after allowing a factor of 30 credit for the aluminum oxide layer. We use a factor of 30 since hydrated oxides are known to form almost immediately on a clean-scraped aluminum surface, and these are both tenacious and self-healing [21].

For both options, 8 $m^3/s$ (1% of the helium flow rate) is processed with a 90% per-pass tritium removal efficiency. Even at 1% of the helium flow rate, 8 $m^3/s$ (17000 CFM) requires a large gas processor.

Combining the two options above with the three cases of tritium input rate from Table 4 gives six representative cases of tritium permeation into the steam/water system. The calculated results are given in Table 7, and range from 55 Ci/day to 11000 Ci/day. It appears that permeation barriers between the helium/steam systems are more effective than between the salt/helium systems. This important fact follows from combining permeation-rate equations to show the dependence on leak-rate coefficients:

$$L_{He} \propto K_{He}(K_{MS})^{1/2} , \qquad (59)$$

i.e., the permeation reduction from the molten salt tubes (see the bottom line in Table 4) is suppressed by the Sievert's Law square-root effect of the next stage. This is unlike the more usual linear effect of staging multiple barriers, where the decontamination factors of each stage multiply directly to give the overall effect.

## 7. Process Concepts for Tritium Recovery from Fluid Loops

Outlined briefly below are some process design concepts for recovering tritium from the three fluid systems; molten salt, helium, and water.

## 7.1 Tritium Recovery from Molten Salt by Flash Vaporization

An estimate of the tritium pressure at the tube outlet is given by Eqs. (36) and and (37). Using the data in Table 4, the result comes to at least 12.9 Torr. This is a very high pressure compared to most breeder designs, and is due to a combination of very low tritium solubility in the salt, moderate wall losses and a reasonably long residence time. A high tritium partial pressure makes recovery relatively easy, and is an important fringe benefit of keeping tritium in the dissolved $T_2$ gas form, rather than as TF.

Figure 5 shows a schematic of the proposed molten salt processing system. We have chosen a flash vaporization unit, similar to the concept of Johnson(20). The liquid enters the vaporizer (or disengager to use Johnson's terminology) and expands through jet nozzles (essentially a showerhead) into a large disengaging tank where liquid droplets settle to a liquid sump at the tank bottom. The pressure in the tank is maintained at the desired level by an external pumping system which carries the effervescing gas out of the chamber. The desired pressure level is set by the design recovery efficiency together with the assumption that residual dissolved tritium in the tank liquid is in equilibrium with the partial pressure of gas-phase tritium. With a design efficiency of 90%, the pressure level would be 1.29 Torr, assuming the temperature in the salt loop is constant and provided there were no other evolved gases. Allowing roughly 3 moles of other gases (primarily helium) per mol of $T_2$ generated(20), the pressure level in the disengager must then be 5.2 Torr. The total gas rate leaving the disengager is essentially 4 times the $T_2$ generation rate, or 2.67 mmols/s. This rate corresponds to a volumetric flow rate of 12.8 ℓ/s at 600°C (3.9 ℓ/min @ 20°C, 1 atm) -

a very modest gas flow rate, even by tritium pumping standards. Assuming that the oxygen level is maintained at a low level with a separate slipstream processor, the 25% $T_2$ in He mixture is cooled to near room temperature, compressed to about 1 atm and passed over a powdered uranium bed to recover the bulk of the tritium as a hydride. The tritium-contaminated helium stream will need a final cleanup step before release, such as the introduction of a little oxygen followed by catalysis/adsorption. The recovery beds will be paralleled, to allow cyclic operation, changeouts, etc.

Returning to the molten salt, we next estimate the pumping requirement. The flash disengager operates at near zero pressure compared to the salt tubes, which at maximum will operate at pressure balance very near to the helium heat transfer loop pressure of 50 atm. At 0.54 $m^3/s$, 50 atm pressure rise, and 70% pump efficiency, the worst-case power requirement is 3.9 MWe (some 500 HP). This does not seem unreasonable, leaving pump technology aside as a separate issue.

The size of the flash disengager is also reasonable at the design recirculation rate for molten salt. Allow a 3 second liquid residence time and a 50% void fraction for gas. This gives a 3.2 $m^3$ tank volume. With a nominal length to diameter ratio of 3, the tank has a diameter of 1.1 m and is 3.3 m high. To give some perspective, the pipe diameter for this salt recirculation loop will need to be in the neighborhood of 0.4 m in order to keep the pressure drop near 1 atm and the pump power less than 0.1 MWe.

It may be helpful to provide the reader a "nearest-integer exponent" cost estimate. This is a very rough estimate; less refined than the back-of-the-envelope method. In our judgment, the molten-salt processor as sketched on Fig. 5 has a nearest-integer exponent of 6, i.e., the capital cost may range from 0.32 to 3.1 M$.

## 7.2 Tritium Recovery from Helium by Oxidation/Adsorption

Tritium can be removed from helium by adding a few ppm oxygen, converting to tritiated water in a packed-bed catalytic reactor, and adsorbing the water vapor on a zeolite molecular seive adsorbent bed[19,22,23]. Two adsorbent beds are required; one on-line while water is being desorbed from the other. The desorbed water then goes to an electrolysis unit for tritium recovery. At 8 $m^3/s$ helium flow, and at 60 atm pressure, the reactor and adsorbers will be substantial vessels, larger than any now in tritium service. Nevertheless, a 90% per-pass recovery should not be difficult. We estimate a nearest-integer cost exponent of 7 for this system.

## 7.3 Tritiated Water Purge or Isotopic Separation

Tritium gas permeating into the steam generation loop will be converted to tritiated water by exchange with the overwhelming supply of hydrogen atoms in hot steam. According to CANDU experience, most of the tritium entering their steam generator leaves as tritium oxide in boiler blowdown and less than 1% as gas or water vapor in turbine off-gas[24]. For simplicity, we will assume the residual HT gas partial pressure is low enough so that permeation loss through condenser-tube walls can be neglected. This means that tritiated water concentration is determined simply by a balance between tritium input and removal rates. Removal may be accomplished either by purging to the environment, as at CANDU, or by processing, as at Grenoble[25].

### 7.3.1 Purge Rate and Concentration for Low Tritium Input Rates

The CANDU purge rate is 7.5% of the steam circulation rate; or 0.06 and 0.10 $m^3/s$ at the Pickering-A and Bruce-A reactors, respectively[24]. Let's suppose that 0.1 $m^3/s$ (1600 GPM) represents a reasonable upper limit on the steam system purge rate. For the lowest tritium input rate shown in Table 7 (55 Ci/d), the steady-state water concentration is 6.4 μCi/ℓ. This is about 300 times the EPA drinking water limit of 20 $\mu Ci/m^3$, which in turn is equivalent to 4 mrem/y for continuous exposure. This modest level of environmental pollution just might prove acceptable, given a long outfall pipe to a large and rapidly moving body of water.

### 7.3.2 Process Rate and Concentration for High Tritium Input Rates

Most of the design options calculated in Table 7 give tritium input rates that will probably prove too high to allow environmental purging to be acceptable by present or future U.S. standards. Excepting case 1A, the range of tritium input rates is from about $10^2$ to $10^4$ Ci/d. If the tritium input was allowed to accumulate in the water system, assuming no losses and with the water mass from Table 5, a concentration level of 1 Ci/ℓ would be reached in only 38 days for the high end of the input range. As discussed earlier, this tritiated water level is a personnel hazard if the steam/water system has <u>any</u> leaks.

Suppose we process water from the steam system at a modest rate of 5 liters per minute and, by isotopic separation, remove 50% of the tritium per pass (we pick these design numbers since a process cost estimate is available). The steady-state concentration depends inversely on the tritium

input rate and will be 0.03, 0.3, and 3 Ci/ℓ for $10^2$, $10^3$, and $10^4$ Ci/d input, respectively. The cost to extract tritium from Savannah River heavy water reactors, using the Grenoble Sultzer Process[25] and for the process conditions above, is about 130 M$ according to the SRP "high spot" estimate[26]. This process involves catalyzed hydrogen gas/water vapor exchange followed by cryogenic distillation of tritium-enriched gas. Since 3 Ci/ℓ tritiated water is very hazardous, as discussed earlier, it may be desirable to increase the process rate for the worst case input to prevent the system from reaching the 3 Ci/ℓ level. This will cause a corresponding increase in process cost. Moreover, the time constant to reach steady state, for the proposed process rate, is only about 4 months.

8. Tritium Inventory in Fluid Systems and Tube Walls

Inventory estimates are summarized in Table 8 for the fluid systems and steel tube walls. The basis for the numbers is discussed below.

Tritium inventory in the molten salt tubes is calculated from

$$I_1 = VH_1\bar{p}_1 \ , \tag{60}$$

where $\bar{p}_1$ is an integral average partial pressure along the length of a reactor tube. We take the average to be $[p(0)+p(\ell)]/2$, use Eq. (35) for $p(0)$, and the $p(\ell)$ values from Table 4. Equation (28) is used for $H_1$, tritium solubility at 680°C in molten salt. Calculated inventories amount to only a fraction of a gram for options A, B, or C. The numbers are small due to the low estimated solubility of tritium in molten salt.

The estimated tritium inventory in the helium system is also small for the three options. Tritium inventory in the water system can range from negligible to large (120 g) over the wide range of tritium input and process rates discussed in paragraphs 7.3.1 and 7.3.2 above.

Tritium inventory in the reactor tube walls is calculated from:

$$I_3 = V[(c/b)^2 - 1]S_3\sqrt{\overline{p_3}}, \qquad (61)$$

where $\overline{p_3}$ is a radial average tritium partial pressure. The solubility of tritium in steel[1] is calculated from:

$$S_3[Ci/(m^3 \cdot Pa^{1/2})] = (1.04E+4)\exp(-705/T[K]) . \qquad (62)$$

The amount of tritium contained in the steel reactor tubes for option A is a large number (200 g) for several reasons. The permeation barrier is on the outside of the tube wall, which keeps the tritium partial pressure in the steel essentially equal to the axial-mean molten salt partial pressure, which is quite high. In addition, tritium solubility in steel is exceptionally high. It is too early in the design cycle to consider this to be a real problem, especially since the whole issue goes away if we put the low-permeability barrier on the inside of the tube.

Options B and C have much lower inventories since there is no tungsten layer and the partial-pressure drop is taken across the molten salt boundary layer, leaving the steel at the relatively-low tritium partial pressure in helium.

The steam generator tubes will store a moderate amount of tritium, somewhat larger than the reactor tubes for options B and C due mainly to the larger wall thickness.

## 9. Summary and Recommendations

Tritium in the form of tritiated water is a personnel hazard at concentration levels well below one part per million, and steam generator water will reach the 1 ppm level within a few months of reactor operation unless a combination of permeation barriers and processing are employed.

To gain a better understanding of permeation effects, equations describing steady-state tritium permeation without axial flow have been derived for a multi-layer tube wall within the blanket region. A layer of frozen salt is included, along with fluid boundary-layer resistances. Calculations of the partial-pressure distribution show significant differences for tubes irradiated at different power densities. Molten salt boundary-layer resistance can be important in the absence of a good permeation barrier, or for a low-power tube coated with a nominal 1 μm tungsten barrier. This nominal permeation barrier will dominate the flow resistance, however, for medium or high power-density tubes closer to the first wall. Examination of the radial flux equation shows a complicated dependence on upstream partial pressure, which reduces to a linear dependence at low pressures where Henry's Law materials become flux limiters and a square-root dependence at high tritium partial pressures where Sievert's Law materials are flux limiting.

An analytical model has been developed to establish the tritium split between wall permeation and reactor-tube flow. The tritium fraction escaping through the tube walls has been quantified for limiting cases of Henry's Law

and Sievert's Law barriers as flux limiters. All parameters of design interest are explicitly included: tritium generation rates and solubility in salt, tube geometry, barrier permeation parameters, and molten salt processing rate and recovery efficiency.

The intermediate helium heat transfer loop has been treated as a well-mixed tank for analytical purposes, with input from the reactor, partial tritium recovery in a slipstream process loop, and Sievert's Law permeation loss to the steam system.

A combination of effective tritium permeation barriers are required on both blanket and steam generator tubes, together with substantial process rates for molten salt and helium systems, in order to hold tritium permeation into the steam system to 55 Ci/d, according to case 1A. If this can be done, it may be feasible to simply purge the steam system of incoming tritium with only minor environmental impact and personnel hazard from steam leaks, and without the necessity of costly and hazardous isotopic processing to separate tritiated and ordinary water.

A surprisingly thin (10 μm) tungsten coating will, in principle, provide a good permeation barrier on the blanket tubes. The feasibility of, in fact, reducing tritium blanket permeation by a factor of 300 or so below the bare steel tube rate for some $10^4$ $m^2$ of tube area will require a research and development effort. Other materials or alloys may prove to be superior, probably at the price of greater thickness of coating.

A relatively thick 1 mm aluminum sleeve was selected to suppress permeation through the steam generator tubes. This gave a calculated reduction factor of more than 500 relative to bare steel, including a factor of 30 due to an assumed oxide layer. This is essentially a brute force approach that may well be improved upon by the development of more sophisticated permeation barriers.

Although we have focused attention on a tungsten barrier due to a remarkably low tritium permeability, beryllium and other low-permeability materials such as ceramics and cermets should be considered in a barrier development problem.

The diffusivity of tritium gas dissolved in molten salt will need to be measured, especially to verify whether or not the fluid boundary-layer barrier of option B is realistic.

Finally, some definitive experimental work on the kinetics of tritium gas conversion to tritiated water at low concentrations in helium is called for. Popular opinion has oscillated over the last decade from an initial optimism that thermodynamics would reduce the gas concentration to nil, to a current pessimism that predicts no gas conversion at all in the main helium loop. The critical experiments remain to be done, both with "clean" walls and particulate-free helium, and in the presence of catalytic surfaces or other reaction promoters. The challenge is to demonstrate a method of drastically reducing tritium gas partial pressure in the intermediate helium loop, and thus suppress permeation into the steam system.

References

[1] Louthan, M. R., Jr., and Derrick, R. G., Corros. Sci. 15, 565, 1975.

[1a] Hassanein, A. M., and Sze, D. K., "Data Survey and Recommended Values for Permeation of Hydrogen and Its Isotopes Through Steel Alloys", unpublished report, Argonne National Laboratory (1984).

[1b] Steward, S. A., "Review of Hydrogen Isotope Permeability Through Materials", Lawrence Livermore National Laboratory Report UCRL-53441 (1983).

[2] Begeal, D. R., J. Vac. Sci. Technol., 15, 1146 (1978)

[3] Guthrie, J. W., et al, J. Nucl. Mater., 53, 313 (1974)

[4] Eichenauer, W. and Pebler, A., Z. Metallkd. 48, 373 (1957)

[5] Jones, P. M. S., and Gibson, R., J. Nucl. Mat. 21, 353 (1967)

[6] Aitken, E. A., et al, Trans. Metall. Soc. AIME, 239, 1565 (1967)

[7] Libby, W. F., "History of Tritium", in Tritium, Moghissi, A. A., and Carter, M. W. (ed.), p. 3, Messenger Graphics, Phoenix, Arizona (1971)

[8] Killough, G. G., Derivation of Dose Conversion Factors for Tritium, Oak Ridge National Laboratory Report, ORNL-5853 (1982)

[9] Sherwood, A. E., Catalytic Oxidation of Tritium in Air at Ambient Temperature, Lawrence Livermore Laboratory Report, UCRL-52811 (1979)

[10] Easterly, C. E. and Bennett, M. R., "Radiation Catalyzed Conversion of Tritium Gas to Tritiated Water", Proc. 5th Topical Meeting on the Technology of Fusion Energy, Knoxville, Tennessee, p. 116, part 2, Nuclear Technology/Fusion 4, No. 2 (1983)

[11] Lewis, G. N., Randall, M., Pitzer, K. S. and Brewer, L., Thermodynamics, Chapter 19, Second Edition, McGraw Hill, 1961.

[12] Malinauskas, A. P., and Richardson, D. M., Ind. Eng. Chem. Fund. 13, 242, 1974.

[13] Shupe, D. S., and Stickney, R. E., J. Chem. Phys. 51, 1620, 1969.

[14] Prausnitz, J. M., Molecular Thermodynamics of Fluid-Phase Equilibria, Chapter 8, Prentice-Hall, 1969.

[15] Eckert, E. R. G. and Drake, R. M. Jr., Analysis of Heat and Mass Transfer, p. 338, 340, 731, McGraw Hill, 1972.

[16] Taylor, G. I., Proc. Roy. Soc. 219A, 186, 1953.

[17] Katsura, H. and Furukawa, K., J. Nucl. Mat. 71, 375, 1978.

[18] Holman, W. R., and Huegel, F. J., Proc. Conf. Chemical Vapor Deposition Refractory Metals, Alloys, and Compounds, p. 127, USAEC (1967)

[19] Bender, D. J., editor, Reference Design for the Standard Mirror Hybrid Reactor, chapter 9, Lawrence Livermore Laboratory and General Atomic Company joint report, UCRL-52478 and GA-A14796, 1978.

[20] Mills, R. G., editor, A Fusion Power Plant, chapters 14 and 15, Plasma Physics Laboratory, Princeton University, Princeton, New Jersey (1974).

[21] S. Steward, Lawrence Livermore National Laboratory, private communication, January, 1984.

[22] Damm, C. C. et al., Preliminary Design of a Tandem-Mirror-Next-Step-Facility, Lawrence Livermore National Laboratory Report UCRL-53060 (1980).

[23] Flanagan, L. A., Steiner, D., and Smith, G. E., Fusion Engineering Device Design Description, Vol. 2, Oak Ridge National Laboratory Report ORNL/TM-7948/V2 (1981).

[24] Wong, K. Y., et al., "Permeation of Tritium Through Steam Generator Tubes at CANDU Stations", 10th Symposium on Fusion Engineering, Philadelphia, December, (1983).

[25] Rae, H. K., editor, Separation of Hydrogen Isotopes, p. 163, ACS Symposium Series 68, Washington, D.C. (1978).

[26] Maienschein, J., Lawrence Livermore National Laboratory, private communication, June 1984.

Table 1. Summary of equations representing tritium permeation data in metals. Most of the data are for hydrogen or deuterium permeation, corrected by the square root of mass ratio. The permeation coefficient is defined by $\phi = DS$, where D is diffusivity and S is solubility. Empirical constants are listed for the equation $\phi = A\exp(-B/T)$, where T is absolute temperature in Kelvin. Conversion from mass to Curies of tritium is based on a specific activity of 9.62E+06 Ci/kg.

| Metal | Permeation equation constants A $Ci/(s \cdot m \cdot Pa^{1/2})$ | B 1/K | Permeation coefficient at 540°C $Ci/(s \cdot m \cdot Pa^{1/2})$ | Data Reference |
|---|---|---|---|---|
| stainless steels | 4.00E-3 | 7200 | 5.71E-7 | (1) |
| copper | 2.82E-2 | 9310 | 3.01E-7 | (2) |
| molybdenum | 2.53E-3 | 8760 | 5.30E-8 | (3) |
| aluminum | 5.98 | 15200 | 4.56E-8 | (4) |
| gold | 5.41E-2 | 13800 | 2.31E-9 | (2) |
| beryllium | 3.37E-9 | 2200 | 2.25E-10 | (5) |
| tungsten | 2.60E-2 | 16600 | 3.54E-11 | (6) |

Table 2. Thermal regime for molten salt reactor tube. Calculated mean temperatures and frozen salt layer thickness for specified heat generation rate and outside helium temperature.

| heat generation rate [MW/m$^3$] | outside helium temp. [C] | mean temperatures [C] | | | | frozen salt layer-thickness [mm] |
|---|---|---|---|---|---|---|
| | | helium boundary layer | stainless steel tube | frozen salt layer | molten salt boundary layer | |
| 60 | 285 | 394 | 504 | 536 | 916 | 0.0805 |
| 20 | 470 | 506 | 543 | 554 | 682 | 0.0875 |
| 6 | 550 | 561 | 572 | 572 | 604 | 0.0 |

Calculations based on a 1/2 inch o.d. tube with a 20 mil wall thickness, a helium-side film coefficient of 7.4E+02 W/(m$^2$•K) based on a packed-bed Reynolds number of 3000, stainless conductivity of 20 W/(m•K), frozen salt conductivity of 0.24 W/(m•K), salt melting point of 565$^o$C, salt-side film coefficient of 2.5E+02 W/(m$^2$•K) based on a molten salt Nusselt number of 4, and well-mixed salt (infinite conductivity) in the central region of the tube.

Table 3. Tritium permeation from molten salt reactor tubes without axial flow.

| Tube distance from plasma centerline [m] | 1.5 | 1.8 | 2.1 |
|---|---|---|---|
| Heat generation rate [$MW/m^3$] | 60 | 20 | 6 |
| Tritium generation rate [$Ci/(s \cdot m^3)$] | 1.24 | 0.414 | 0.124 |
| Tritium partial pressure in molten salt [Pa] | $6.31 \times 10^4$ | $3.03 \times 10^3$ | $1.27 \times 10^3$ |
| Tritium partial pressure drop [% of total]: | | | |
| molten salt boundary layer | 1.7 | 62.6 | 98.2 |
| frozen salt layer | 1.2 | 7.1 | 0.0 |
| stainless steel tube wall | 3.6 | 2.0 | 0.2 |
| tungsten coating (1 μm) | 93.5 | 28.3 | 1.6 |
| helium gas boundary layer | 0.0 | 0.0 | 0.0 |

Calculated values based on Table 2 thermal parameters and frozen-salt layer thicknesses. Tritium generation rate is scaled to the tube heat-generation rate, and 100% permeation is assumed through the tube walls (no axial flow). Tritium partial pressure assumed to be $10^{-2}$ Pa in Helium coolant.

Table 4. Permeation from the molten salt loop for three design options

| parameter | Design option A | B | C |
|---|---|---|---|
| n | 0.9 | 0.9 | 0.0 |
| $\ell/U$, s | 120 | 120 | - |
| (d-c), μm | 10 | - | - |
| $p_{max}$, Pa | 2710 | 2710 | 3050 |
| α | 0.0759 | 0.367 | 1.000 |
| $p(\ell)$ | 2500 | 1720 | 3050 |
| $L_{MS}$, Ci/s | 2.94 | 14.2 | 38.7 |

For all cases: $G = 0.596$ Ci/(s·m$^3$)
$V = 65$ m$^3$
$b = 5.842$ mm

Table 5. Size comparison of molten salt reactor processing and coolant[a] loops.

| | Molten Salt | Helium | Steam/Water |
|---|---|---|---|
| mass [kg] | $4.6 \times 10^5$ | $1.3 \times 10^4$ | $3.8 \times 10^5$ |
| volume [$m^3$] | 100 | 3200 | 10000 |
| @ T [C] | 600 | 450 | 340 |
| @ P [MPa] | 5.1 | 6.1 | 8.4 |
| mass flow rate [kg/s] | $2.5 \times 10^3$ | $3.2 \times 10^3$ | $1.6 \times 10^3$ |
| volume flow rate [$m^3/s$] | 0.54 | 800 | 43 |

[a] Coolant loop flow rate data from reference [19], mass and volume are estimates.

Table 6. Tritium permeation through bare-steel helium/steam heat exchangers. Based on data in reference [19] for 4480 MWt design heat duty. Data shown are for one generator set, except for bottom row which is for the reactor (12 generators). Permeation coefficient, DS, is from reference [1].

| Type | Area [$m^2$] | Area (%) | wall thickness [mm] | mean temp. [C] | DS[d] | Leak rate coefficient[e] | Leak rate coefficient (%) |
|---|---|---|---|---|---|---|---|
| resuperheater | 512 | (15) | 2.54 | 488 | 27.1 | $5.46 \times 10^3$ | (46) |
| superheater | 385 | (12) | 1.78 | 432 | 12.8 | $2.77 \times 10^3$ | (23) |
| evaporator | 1409 | (42) | 1.57 | 355 | 3.66 | $3.28 \times 10^3$ | (27) |
| economizer | 1017 | (31) | 1.57 | 275 | 0.678 | $0.445 \times 10$ | ( 4) |
| 1 generator | 3323 | (100) | | <384>[b] | <6.11>[c] | $1.20 \times 10^4$ | (100) |
| 1 reactor (x12) | $3.99 \times 10^4$ | | | | | $1.44 \times 10^5$ | |

a Note that 46% of the leakage goes through only 15% of the area, and 69% of the leakage goes through only 27% of the area.

b permeation mean temperature calculated from weighted mean DS; footnote c.

c weighted mean $DS = \Sigma(DS_j A_j/W_j)/\Sigma(A_j/W_j)$ .

d permeation coefficient for clean steel (no oxide) at the specified temperature. [$Ci \cdot mm/d \cdot m^2 \cdot Pa^{1/2}$).

e leak rate coefficient units are [$Ci/(d \cdot Pa^{1/2})$].

*Table 7. Tritium permeation rate into the steam/water system for different combinations of design options.*

| design option | $L_{He}$ [Ci/d] |
|---|---|
| 1 - process helium, 1 mm aluminum sleeve, with: | |
| A - process molten salt, 10 μm tungsten coating | 5.5 E+1 |
| B - process molten salt, fluid b.l. resistance only | 1.2 E+2 |
| C - molten salt not processed, 100% permeation | 2.0 E+2 |
| 2 - process helium, steel tube resistance only, with: | |
| A - same as above | 3.0 E+3 |
| B - same as above | 6.5 E+3 |
| C - same as above | 1.1 E+4 |

Tritium input to the helium system is taken from Table 4 for options A, B, and C. Partial pressure in helium is calculated from Eq. (56) with n = 0.9, g = 0.01, $Q_5$ = 800 $m^3/s$, $H_5$ = 6980/T[K] Ci/($m^3$·Pa), and T = 723 K. The result is 4.2E-2, 2.0E-1, and 5.5E-1 Pa for options A, B, and C, respectively.

Table 8. Tritium inventory in fluid systems and steel tube walls.

| | Tritium inventory [g] | | |
|---|---|---|---|
| (option:) | (A) | (B) | (C) |
| Molten salt system[a] | 0.4 | 0.3 | 0.6 |
| Helium gas system[b] | 0.1 | 0.6 | 1.8 |
| Steel walls of molten salt reactor tubes[c] | 200. | 2.4 | 4.0 |
| Steel walls of steam generator tubes[d] | 5.1 | 11. | 19. |
| (tritium input rate to steam/water system, [Ci/d]:) | ($10^2$) | ($10^3$) | ($10^4$) |
| Water system[e] | 1.2 | 12. | 120. |

a For options A and B a 100 $m^3$ salt volume is used to allow for the process loop, while option C uses only 65 $m^3$.

b Based on Table 5 helium volume and the tritium partial pressures given in the footnote to Table 7.

c Based on 1/2 inch o.d. tubes with 20 mil wall thickness, tritium solubility from reference [1] @ 540°C, and partial pressures from Tables 4 and 7.

d Based on Table 6 tube sizes and temperatures, weighed according to $\sum A_j W_j S_j$, with tritium partial pressures given in the footnote to Table 7. Values given are for options 1A, 1B, and 1C. For 2A, 2B, and 2C divide by 2.

e Based on Table 5 water volume and tritiated water concentrations given in sections 7.3.2. For the low-input purge case of 7.3.1, the inventory is only 2.5E-4 g.

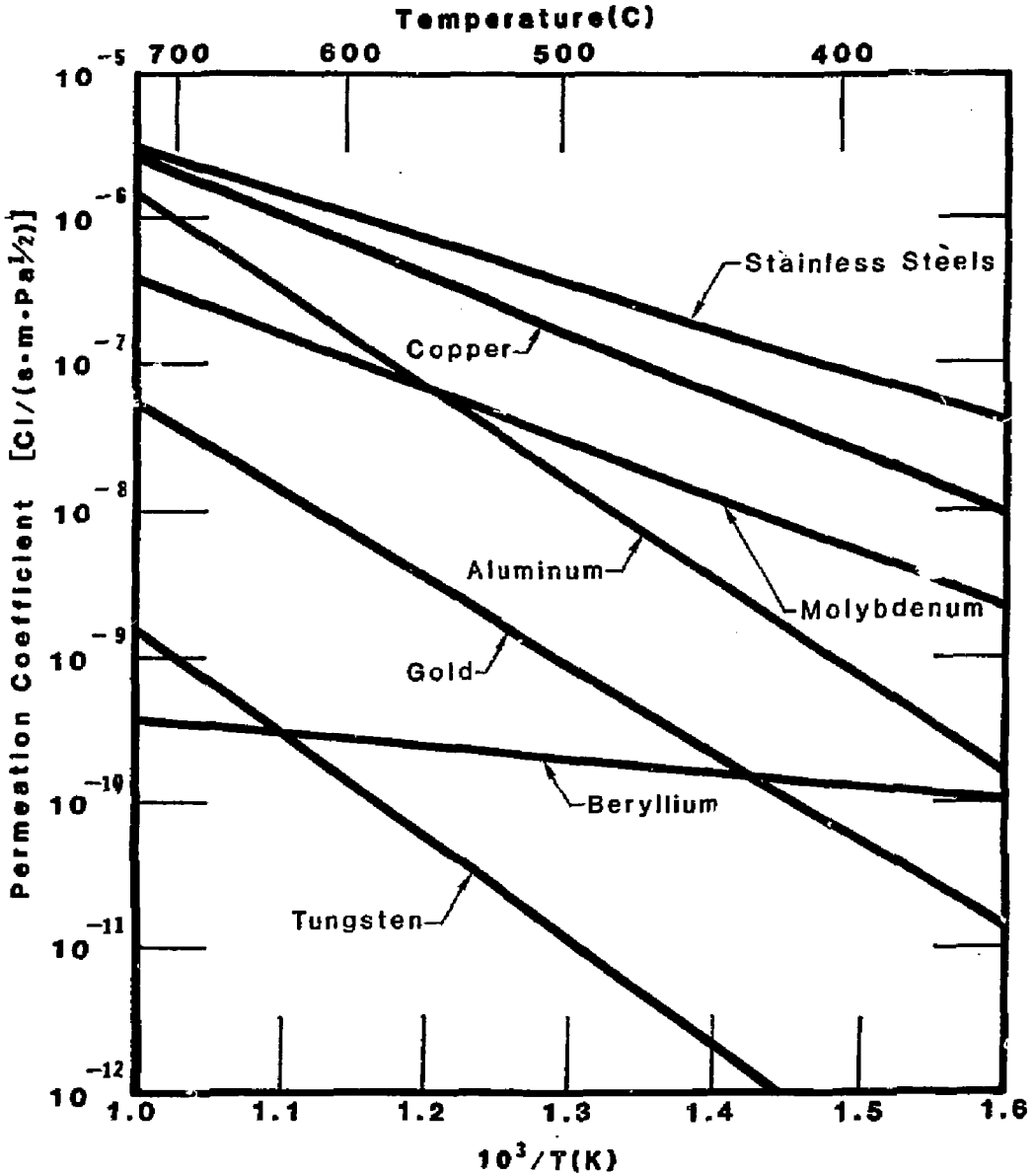


Figure 1. Permeation coefficient of tritium through metals.

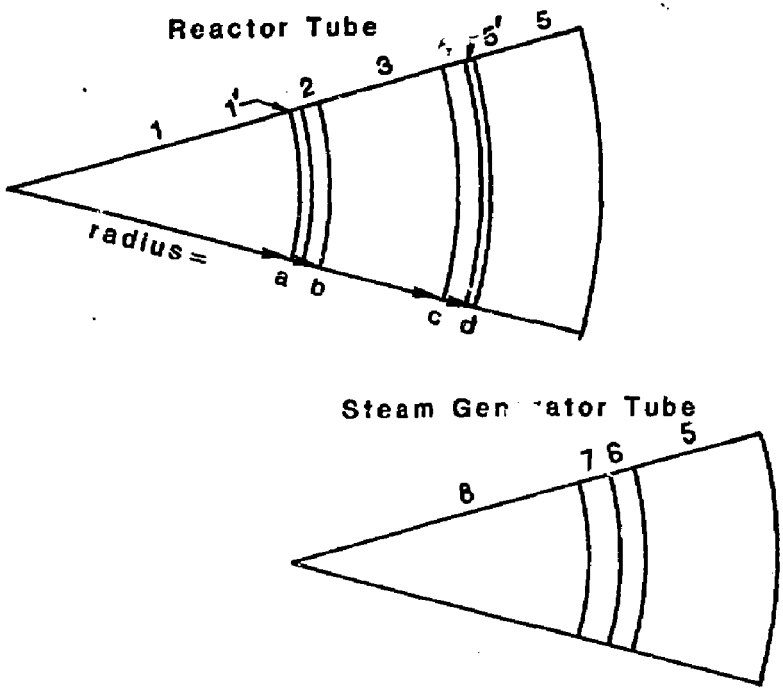


Figure 2. Permeation Geometry and Materials

Reactor Tube:

| | |
|---|---|
| 1 | molten salt |
| 1′ | molten salt boundary layer |
| 2 | frozen salt |
| 3 | stainless steel tube |
| 4 | permeation barrier (tungsten) |
| 5′ | helium gas boundary layer |
| 5 | helium gas |

Steam Generator Tube:

| | |
|---|---|
| 5 | helium gas |
| 6 | stainless steel tube |
| 7 | permeation barrier (aluminum) |
| 8 | water/steam |

Figure 3. Model for tritium split in reactor tube. Molten salt flows at velocity U, and is well-mixed radially. Local tritium partial pressure at z, p(z), drives the radial permeation flux F(p).

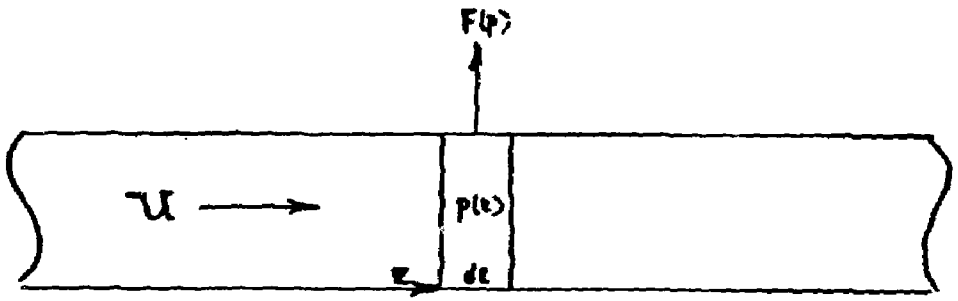

Figure 4. Schematic diagram of tritium processing loops. Only principal flows shown. Losses from process lines, and equipment housings not shown.

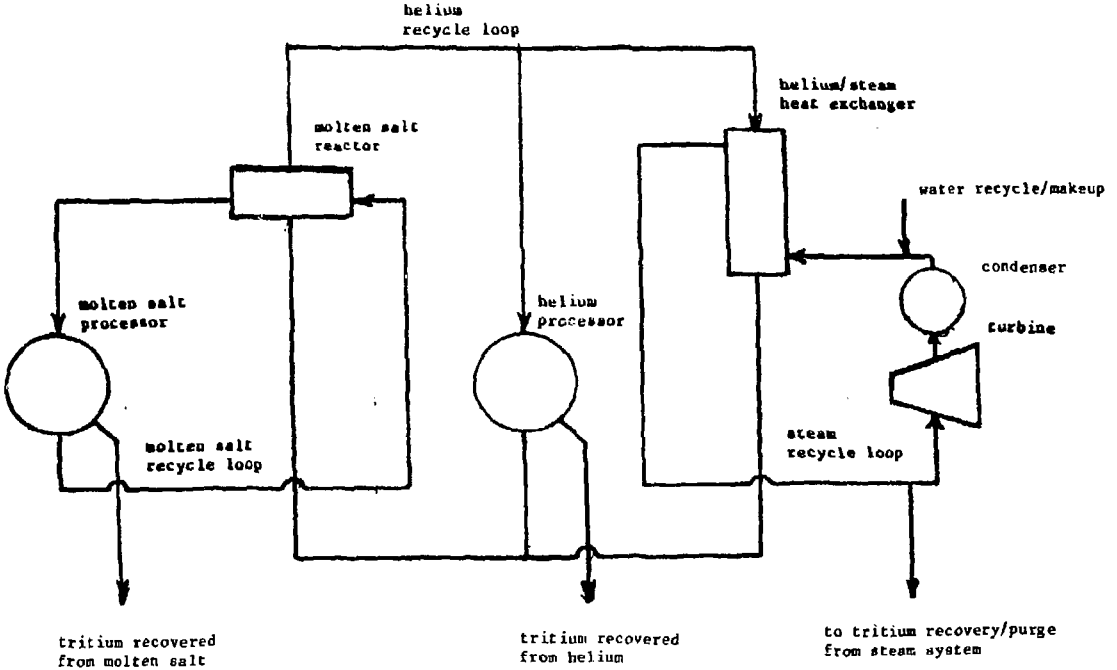

Figure 5. Molten Salt Tritium Processing